Published in final edited form as:
Auton Neurosci. 2006 January 30; 124(1-2): 81–89. doi:10.1016/j.autneu.2005.12.001.

Loss of parasympathetic innervation leads to sustained expression of pro-inflammatory genes in the rat lacrimal gland

Doan H. Nguyen[a,*], **Venu Vadlamudi**[a], **Hiroshi Toshida**[b], and **Roger W. Beuerman**[a,c]

[a]LSU Eye Center/Lions Eye Research Laboratories, Department of Ophthalmology, Laboratory for the Molecular Biology of the Ocular Surface, Louisiana State University Health Sciences Center, 2020 Gravier Street, Suite B, New Orleans, LA 70112, United States

[b]Juntendo University School of Medicine, Department of Ophthalmology and Pharmacology, Tokyo, Japan

[c]Singapore Eye Research Institute, Singapore 168751, Singapore

Abstract

It has been shown that removal of parasympathetic innervation to the lacrimal gland (LG) leads to rapid reduction in tear flow. Additionally, removal of the neural input resulted in disorganization of LG structure and changes in the expression of genes associated with the secretory pathway and inflammation. The goal of this study was to investigate the change in pro-inflammatory and pro-apoptotic gene expression in the rat LG following parasympathetic denervation. Male Long- Evans rats underwent unilateral sectioning of the greater superficial petrosal nerve and were sacrificed 7 days or 2.5 months later. cDNA was synthesized from LG RNA from the contralateral control (Ctla) and parasympathectomized (Px) glands and comparative real-time PCR was performed. Mean threshold cycles (MC_T) for the Ctla and Px LG genes were normalized to 18S rRNA MC_T values, and the relative fold change was calculated for each gene using the $2^{-\Delta\Delta C}_T$ method. The expression of nuclear factor kappa B1, caspase 1, eotaxin, leukocyte antigen MRC-OX44, allograft inflammatory factor-1, MHC class II molecules RT.1B and RT.1D, IgG receptor FcRn, and macrophage metalloelastase was increased and remained elevated in the Px LG, compared with the Ctla LG. Increased expression of the initiator of apoptosis gene, caspase 2, was confirmed, but expression of the executor gene, caspase 6, was not elevated in the Px LG. Reduced expression of genes associated with post-translational protein processing-furin convertase, protein disulfide isomerase, and UDP-gal transporter isozyme 1-was noted in the Px LG. No significant changes in the expression of genes associated with lysosomal and non-lysosomal-mediated protein degradation were found. Removal of parasympathetic input may lead to decreased capacity for protein synthesis and elevated immune responses in the Px LG. These changes occur without increases in expression of the muscarinic acetylcholine receptor subtype 3, and may suggest the early changes in LG acinar cells and the pathophysiology of autoimmune responses.

Keywords

Rat; Lacrimal gland; Muscarinic; Parasympathetic; Dry eye; Inflammation; Apoptosis

*Corresponding author. Tel.: +1 504 412 1200x1428; fax: +1 504 412 1315. *E-mail address:* E-mail: dnguye@lsuhsc.edu (D.H. Nguyen)..

1. Introduction

The lacrimal gland (LG) and the ocular surface are linked through the central nervous system by sensory and peripheral autonomic neural systems. The secretion of LG proteins into the pre-ocular tear film contributes to the maintenance of the ocular surface and its homeostasis, and is mediated mainly by activation of the muscarinic parasympathetic neural pathway (Stern et al., 2004). Sensory and sympathetic nerves are also found in the LG, but they are not as densely distributed as parasympathetic nerves (Hodges and Dartt, 2003). The release of norepinephrine from activation of sympathetic nerves also stimulates protein secretion from LG. Elimination of parasympathetic regulation in the rabbit by sectioning of the greater superficial petrosal nerve (GSPN) results in rapid reduction of tear flow (Toshida and Beuerman, 2002). Similarly, 7 days after the GSPN was sectioned unilaterally in the rat, severe dry eye, corneal ulceration, and disorganization and dissolution of LG structure was seen on the parasympathectomized (Px) side, whereas on the contralateral, unoperated control (Ctla) side, the LG remained normal. The LG from the sham-denervated animals were similar to the Ctla LG. Subsequent gene expression analysis of the Ctla and Px LG by DNA microarray found increased expression of pro-inflammatory, pro-apoptotic, and immune regulatory genes in the Px LG (Nguyen et al., 2004).

Aside from the secretory parenchymal constituents of the LG, a small population of immune cells (plasma cells, macrophages, and T-lymphocytes) is also normally found in the LG (Walcott et al., 1994). The numbers of these immune cells increase during normal aging and more dramatically in autoimmune disorders, including Sjögren's syndrome (Gudmundsson et al., 1988; Mircheff et al., 1991; Williams et al., 1994; Obata et al., 1995). Moreover, it has also been demonstrated that the acinar epithelial cells are active participants in the initiation and progression of LG inflammation and the immune response in the LG (Mircheff et al., 1991). In the absence of a systemic immune disorder, primary LG dysfunction may be manifested by alterations to the neural and endocrine mechanisms, which alter the secretory function of the LG (Sullivan, 1999). Based on these studies, as well as our previous DNA microarray analysis studies showing an increase in the expression of pro-inflammatory and proapoptotic mediators after GSPN sectioning (Nguyen et al., 2004), it is plausible that alteration of muscarinic parasympathetic input and the LG secretory apparatus may be an early initiation factor for activating an immune response in the LG, but further investigation and verification are warranted.

In recent years, topical immunosuppressive drugs such as cyclosporine A have demonstrated considerable benefits in the treatment of severe dry eye (keratoconjunctivitis sicca) (Pflugfelder, 2004). The biological action of cyclosporine A has been suggested to occur via a mechanism that controls inflammation associated with the production of pro-inflammatory cytokines on the ocular surface and in the LG (Gao et al., 1998b). Moreover, it has been proposed that limiting tissue damage associated with chronic inflammation is related to suppression of apoptosis of ocular surface cells and, possibly, LG acinar cells as well (Gao et al., 1998a). Apoptosis, or programmed cell death, is a genetically controlled, physiological process essential for normal tissue development and homeostasis. The best-known mediators of apoptosis are the caspases, which are *c*ysteine-dependent, *asp*artate-specific prote*ases* involved in pro-inflammatory cytokine activation and are the effectors of apoptotic pathways (Creagh et al., 2003). Recently, inhibition of conjunctival epithelial apoptosis has been proposed to be the key mechanism of action related to the therapeutic effect of cyclosporine A (Strong et al., 2005). These ideas are congruent with evidence of increased caspase expression and apoptotic cell death in corneal and conjunctival epithelial cells in dry eye in humans (Tsubota et al., 2003) and also in various animal dry eye models (Gao et al., 1998a,b; Yeh et al., 2003). Thus, a fundamental understanding of apoptotic events, including potential triggers and modulators of this activity in dry eye, is essential in developing targeted therapy.

Rapid implementation and improvement of DNA microarray technology over the past few years have been valuable in providing a whole genome approach to gene expression analysis (King and Sinha, 2001). Although these advances in genome-level analysis of experimental and naturally occurring conditions and models have been remarkable, recent reports have shown that secondary methods are required to validate results from DNA microarray analysis (Rajeevan et al., 2001a,b; Jenson et al., 2003). Numerous studies have shown that, of the several methods commonly used to quantify mRNA levels, real-time PCR offers the greatest reliability and sensitivity for both quantitative and relative comparisons (Rajeevan et al., 2001a,b; Ramakers et al., 2003; Radoniæ et al., 2004). Previously, we used real-time PCR to verify the results obtained from DNA microarray analysis (Nguyen et al., 2003), an approach that has also been reported in other studies (Rajeevan et al., 2001a,b). In the present study, we examined the expression levels of several pro-inflammatory, pro-apoptotic, and immune regulatory genes in the LG following the loss of muscarinic parasympathetic regulation. Our results lead us to conjecture that muscarinic parasympathetic stimulation is critical not only for the maintenance of LG structural organization, but also for the regulation of immune homeostasis of the LG. The loss of this neural control may lead to a persistent and chronic inflammatory state that results in a progressive loss of LG acinar cell function and apoptosis of acinar cells.

2. Materials and methods

2.1. Pre-ganglionic parasympathetic denervation

Male Long-Evans rats (200-250 g) were purchased from Harlan Laboratories (Indianapolis, IN) and controlled pre-ganglionic parasympathetic denervation was carried out as previously described (Nguyen et al., 2004). All animal studies were carried out in accordance with the ARVO Statement on the Use of Animals in Research in Vision and Ophthalmology and with approval from the Louisiana State University Health Sciences Center Institutional Animal Care and Use Committee (IACUC). In brief, several millimeters of the GSPN were sectioned and removed using an auditory meatus approach, as previously performed in the rabbit (Toshida and Beuerman, 2002). Seven days (short-term) or at 2.5 months (long-term) after surgery, animals were sacrificed and the superior LG was removed through a skin incision from the Ctla and Px sides. LG tissues were frozen immediately in liquid nitrogen.

2.2. Total RNA extraction and cDNA synthesis

Total RNA from the Ctla and Px LG ($n = 3$) was extracted using the RNeasy Mini Kit (Qiagen Inc., Valencia, CA) according to the manufacturer's instructions and as previously described (Nguyen et al., 2004). RNA quality was determined by spectrophotometry and all RNA samples had an A_{260}/A_{280} ratio of 1.9 or greater. In a further assessment of RNA quality, a 5 μg sample was denatured and separated on a 1% formaldehyde agarose gel stained with ethidium bromide and photographed under UV illumination using the Eagle Eye II Still Video System and software (Stratagene, La Jolla, CA). First-strand cDNA synthesis was carried out with 1 μg of total RNA using the iScript cDNA Synthesis Kit (Bio-Rad Laboratories, Hercules, CA) and all reactions were carried out in a Programmable Thermal Controller (MJ Research Inc., Waltham, MA).

2.3. Primer design and real-time PCR

Genes of interest that were found to be differentially expressed by DNA microarray analysis (Nguyen et al., 2004) were selected for validation by real-time PCR. Genespecific primers and TaqMan probes were designed using Beacon Designer 2.0 (Premier Biosoft International, Palo Alto, CA) and purchased from the LSU Health Sciences Center Core Laboratories and Integrated DNA Technologies (Coralville, IA). The lengths of amplicons ranged from 90 to 283 base pairs. Table 1 lists the primer and TaqMan probe sequences employed in this study.

Real-time PCR was carried out using the iCycler iQ Real-time PCR Detection System (Bio-Rad). The threshold cycle (C_T) for each real-time PCR reaction was determined using the default settings of the iCycler software (Version 3.0, Bio-Rad). PCR reactions were first tested for each gene using rat brain and rat spleen cDNA as positive controls and RNase-free water as a negative control to explore optimal annealing and melting temperatures. The 18S rRNA was used as an endogenous control gene and run in separate reactions in triplicate over a threefold dilution series. Melting curve analysis was carried out immediately after the PCR amplification to ensure specificity and uniformity of the amplicon. Upon completion of the melting curve analysis, a 10-μL aliquot was analyzed on a 2% agarose gel stained with ethidium bromide. A 1-μg equivalent of φX174 DNA-Hae III Digest (New England BioLabs, Inc., Beverly, MA) was used as a molecular size ladder. The gel was photographed under UV illumination using the Eagle Eye II Still Video System and software.

For genes tested using SYBR Green I DNA-binding chemistry, reactions were carried out in a 25-μL final volume containing 12.5 μL of iQ SYBR Green Supermix (BioRad), 200 nM each of sense and antisense primers, and 1.5 μL of cDNA sample. A master mix was prepared for each gene, and all reactions were run in triplicate. The amplification program consisted of a one cycle “hot-start” of 95 °C for 2 min, followed by a two-step amplification of 40 cycles at 95 °C for 10 s and 50-60 °C annealing for 20-30 s. Melting curve and agarose gel analyses of the reactions were used to confirm that the correct product was amplified.

For genes analyzed using primers and a TaqMan probe, reactions were also carried out in a 25-μL final volume. A master mix was made as described above, except for the use of 12.0 μL of iQ Supermix (BioRad) and the addition of 0.5 μL of TaqMan probe (10 μM). Melting curve analysis was unavailable for reactions using TaqMan probes, so agarose gel analysis of the amplicon was performed using a 2% agarose gel, as described above.

2.4. Real-time PCR data analysis

Real-time PCR C_T data were analyzed using the $2_{\tau}^{-\Delta\Delta C}$ and $2^{-\Delta C'_{\tau}}$ methods as described by Livak and Schmittgen (2001). For the genes tested using SYBR Green I DNA-binding chemistry, the $2_{\tau}^{-\Delta\Delta C}$ method was employed for data analysis as normalization to the 18S rRNA was directly applicable. By this methodology, the calculation of $\Delta\Delta C_T = (C_{T,target} - C_{T,reference})_{Px} - (C_{T,target} C_{T,reference}$ Ctla allows for the relative quantification of mRNA levels in the Px samples, compared with the normally innervated Ctla samples, in each rat, normalizing to the reference (endogenous control) gene. However, for the genes tested using TaqMan probes, we employed the $2^{-\Delta C'_{\tau}}$ method for fold-change calculation. By this method, the Ctla and Px C_T values for each gene are directly compared to one another without normalization to the reference gene; because the C_T data of the 18S rRNA in the Ctla and Px cDNA samples were not different, differences in the C_T data between the two conditions revealed increases or decreases in the gene of interest. Validation was defined as a change greater than or equal to a twofold change by both real-time PCR and DNA microarray analyses or when fold change from real-time PCR data exceeded that of microarray analysis. Statistical analysis was carried out on the C_T values for each of the genes ($MC_T \pm$ S.E.M.) using the Student's *t*-test (Statistica 6.0, StatSoft Inc., Tulsa, OK) (Table 2).

3. Results

3.1. Real-time PCR

The data from real-time PCR consisted of threshold cycle (C_T) values which were compared for the Ctla and Px LG. The C_T is obtained from the log-linear phase of the PCR reaction and is inversely related to the amount of the initial template nucleic acid present in the sample. Thus the larger the C_T value, the smaller the amount of original starting material (Walker,

2002). Data were reported as the mean of the C_T values (MC_T) for the Ctla and Px LG samples from triplicate experiments for each gene (Table 2). To ensure that the 18S gene was a suitable endogenous control, we tested serial dilutions over a threefold range and found no statistically significant difference in the MC_T values for the Ctla and Px LG samples (Table 3). The standard curve of the dilution series had r^2 values of 0.9877 and 0.9882 for the Ctla and Px samples, respectively, which confirmed that the 18S gene MC_T values were linear over the threefold dilution series (Fig. 1).

3.2. Gene expression profile in short-term parasympathectomized rats

To validate the data from the previous DNA microarray analysis, we calculated the fold change for each gene using the real-time PCR data. Because the C_T carries an intrinsic quantitative value, we employed the $2_T^{-\Delta\Delta C}$ method for fold-change calculation as described by Livak and Schmittgen (2001). This method compares the C_T of the gene of interest in the sample with that of the endogenous control, 18S rRNA. To use this method, amplification efficiency had to be nearly the same for each sample, i.e., between each gene and the 18S rRNA control gene. Because of our optimization of each reaction before using vital samples, we were able to achieve equivalent amplification efficiencies for the genes tested and the 18S rRNA. A modified version of the $2_T^{-\Delta\Delta C}$ method, the $2^{-\Delta C'_T}$ method, also described by Livak and Schmittgen (2001), was employed for fold-change calculations of genes utilizing TaqMan probes. These genes included protein disulfide isomerase (PDI), eotaxin, and caspase-1 (also known as interleukin-1β converting enzyme). By this method, C_T values for each gene in Px and Ctla LG samples were directly compared with one another. Fold-change calculations from real-time PCR were compared with those from previous DNA microarray analysis. Validation of gene expression levels is presented in Table 4.

Of the 11 pro-inflammatory and pro-apoptotic genes-eotaxin, caspase-1 (interleukin-1β converting enzyme; ICE), caspase-2 (Nedd2/Ich-1), caspase-6 (Mch2), leukocyte antigen MRC-OX44 (CD53), IgG receptor FcRn large subunit p51, MHC class II antigen RT1.D alpha chain, MHC class II antigen RT1.B beta chain, macrophage metalloelastase (MME), NF-κB1, and allograft inflammatory factor-1 (AIF-1)-selected for real-time PCR analysis, 10 genes were found to be differentially expressed based on the criteria mentioned, giving a confirmation rate of 91% for DNA microarray results. However, the expression fold changes obtained from microarray analysis and real-time PCR validation varied substantially, regardless of the chemistry used for real-time PCR quantification. Of the seven genes involved in protein processing, only three genes were validated by real-time PCR—protein disulfide isomerase (PDI), furin convertase, and UDP-galactose transporter related isozyme 1 (UDP-Gal). The expression levels of these genes were significantly reduced ($P < 0.05$), as was previously found by DNA microarray analysis (Nguyen et al., 2004). The four genes whose expression was found to be elevated in the denervated gland by DNA microarray-proteasome subunit, beta type 4 (PSMB4), proteasome RC1 subunit (PSMB8, LMP7), lysosomal acid lipase (LAL), and lysosomal membrane glycoprotein (LAMP-1)-were not validated by real-time PCR. Finally, expression of the M_3R was not found to be altered, as has been previously reported (Nguyen et al., 2004).

3.3. Pro-inflammatory gene expression in long-term parasympathectomized rats

Several pro-inflammatory and immune regulators that were found to be elevated in the denervated LG after 7 days were further analyzed in the LG of rats that had undergone long-term parasympathectomy (2.5 months). Tear secretion in these long-term denervated animals remained lower on the denervated side, compared with the contralateral control side (Nguyen et al., 2005). The expression of all of these selected genes, including caspase-1, macrophage metalloelastase, NF-κB1, AIF-1, FcRn, and MHC class II molecules RT1.D and RT1.B,

remained elevated (greater than twofold) in the denervated gland, compared with the control gland (Table 5). When the expression levels in the long-term denervated specimens were compared with those of the 7-day denervated specimens, all genes showed comparable fold-change increases. However, the levels of expression of both of the MHC class II molecules were approximately threefold higher after 2.5 months of denervation than after 7 days of denervation.

4. Discussion

4.1. Expression of genes associated with protein processing

The seven genes associated with protein processing can be divided into two functional groups. The three genes that exhibited reduced expression (PDI, furin convertase, and UDP-Gal) are associated with the secretory apparatus and the post-translational modification of newly synthesized proteins for export. The other four genes (PSMB4, PSMB8, LAL, and LAMP-1) are commonly associated with protein degradation and endosomal proteolysis; expression of these genes was not elevated in the Px gland. Expression of the two lysosomal-associated marker proteins (LAL and LAMP-1) was also not elevated, suggesting that lysosomal activity may not yet play a prominent role in the denervated LG at this early time point (7 days). In addition, the absence of significantly increased expression of PSMB4 and PSMB8 suggests that proteasome-mediated degradation of damaged or misfolded proteins was not activated. This finding, coupled with the decreased expression of PDI, furin, and UDP-Gal, suggests a possible reduction in post-translational activities in the endoplasmic reticulum (ER) and Golgi apparatus, as well as in the ER-associated degradation (ERAD) pathway. The decreased expression of PDI argues against the activation of an ER-stress response, in that an activated ER-stress response would lead to an increase in the expression of PDI in response to the accumulation of unfolded or misfolded proteins (Rutkowski and Kaufman, 2004). In short, these results suggest that it is the ER-processing of newly synthesized proteins that is diminished, not the degradation component, following loss of parasympathetic input in the denervated LG.

4.2. Expression of genes associated with pro-inflammatory and immune regulation

Among the upregulated pro-inflammatory genes, eotaxin and allograft inflammatory factor-1 (AIF-1) are generally classified as chemotactic and activator proteins, produced by both epithelial cells and macrophages (Utans et al., 1995; Coillie et al., 1999; Sabroe et al., 2002). The increased expression of these chemotactic activators, along with the increased expression of MME, a macrophage-specific matrix metalloproteinase, suggests that monocyte/macrophage lineage cells participate in tissue reorganization in the denervated LG (Nguyen et al., 2004).

The increased expression of the leukocyte antigen MRC-OX44 provides additional evidence for a pro-inflammatory state and possibly recruitment of immune cells to the denervated LG. The MRC-OX44 surface antigen is a member of the tetraspan membrane protein family that mediates the response of monocytes and B-cells (Berditchevski, 2001). These tetraspan membrane proteins form a multiprotein complex with β1-integrin and MHC antigens to enhance cell adhesion and migration during antigen presentation to T cells.

The increased and sustained expression of the MHC class II molecules, RT1.D alpha chain and RT1.B beta chain, which are the rat orthologs of HLA-DRA and HLA-DQB, respectively, suggests an altered immune response similar to that seen in autoimmune diseases. The acinar epithelial cells are also active participants in this pathological process and can be induced to express MHC class II molecules (Mircheff et al., 1991).

Increased expression of NF-κB1, a gene coding for the p105 precursor isoform which may undergo further post-translational processing to generate the active p50 isoform, was observed (Lin et al., 2000). The NF-κB1 (p50) binds to the p65 RelA to form the NF-κB complex that activates the transcription of numerous pro-inflammatory genes. The p105 isoform also functions as an important inhibitor of NF-κB activity (Ishikawa et al., 1998). Hence, the homeostatic balance of p105 and p50 appears to be an important factor in the control of inflammation.

Increased and sustained expression of the IgG receptor FcRn large p51 subunit provides further evidence of elevated immune responses in the denervated LG. The FcRn (FcR neonatal) receptor is a member of the MHC class I protein family. It is made up of the large p51 subunit and a small β2-microglobulin p14 subunit and participates in the control of serum-IgG levels (Raghavan and Bjorkman, 1996). The increased expression of FcRn may be a response to elevated levels of serum IgG and the increase in the humoral immune response in the denervated LG (Akilesh et al., 2004).

4.3. Expression of genes associated with apoptosis: caspase-1, -2, and -6

Caspase-1, although classified as a member of the caspase family, is more commonly associated with inflammation. Caspase-1 activates the pro-inflammatory cytokines interleukin-1β (IL-1β), interleukin-1α (IL-1α), and interleukin-18 (Creagh et al., 2003). The increased expression of caspase-1 in the denervated gland suggests an increase in the proteolytic activation of pro-inflammatory cytokines, as has been reported for increased IL-1α and IL-1β in the tears of dry eye patients (Solomon et al., 2001).

The expression of caspase-2 (Nedd2/Ich-1) was also increased in the denervated glands, compared with the control glands. Caspase-2 is regarded as an initiator caspase, and may be activated by changes in mitochondrial integrity and cytochrome c release (Creagh et al., 2003; Slee et al., 1999). In contrast, the expression of the executor, caspase-6, was not changed with denervation. These results suggest that caspase-mediated apoptotic cell death may not be prominent at this early time period (7 days) after denervation, although alternative pathways for activating other executor caspases may be involved. Recent work by Tsubota et al. (2003) suggests that early apoptosis of lacrimal acinar cells may explain, in part, some of the aspects of glandular dysfunction, as opposed to later stages where lymphocyte infiltration and Fas-FasL interactions probably affect the major mechanisms leading to lacrimal gland dysfunction (Tsubota et al., 2003). In our rat dry eye model, we did not observe any evidence of lymphocytic infiltration 7 days after parasympathectomy, lending greater credence to the idea of an early state of inflammation prior to initiation of apoptosis.

5. Conclusions

Our results verify that parasympathetic innervation may regulate some aspects of ER-resident protein expression in LG acinar cells. Moreover, the expression of pro-inflammatory and immune mediators is also affected by loss of this input, and the effect is more pronounced after 2.5 months. Although our previous study did not show typical apoptotic changes on microscopic examination, the pattern of increased expression of some members of the caspase family suggests that this process may have been initiated in the Px LG 7 days after parasympathectomy. The temporal relationship between these processes has not been elucidated and may require further examination of earlier time points. Finally, the increased expression of pro-inflammatory, proapoptotic, and immune mediators occurs in the absence of any significant increases or decrease in the expression of the M3 muscarinic receptor (Nguyen et al., 2004) and may be caused by loss of activation of the main neural pathway for lacrimal gland secretion.

Acknowledgments

This work was supported in part by USPHS Grants R01EY012416 (RWB) and P30EY002377 (LSU Eye Center Core grant) from the National Eye Institute, National Institutes of Health, Bethesda, Maryland and an unrestricted challenge grant (LSU Eye Center) from Research to Prevent Blindness, New York, New York. This publication was made possible by NIH Grant Number P20 RR16456 from the BRIN/INBRE Program of the National Center for Research Resources. Its contents are solely the responsibility of the authors and do not necessarily represent the official views of NIH.

References

Akilesh S, Petkova S, Sproule TJ, Shaffer DJ, Christianson GJ, Roopenian D. The MHC class I-like Fc receptor promotes humorally mediated autoimmune disease. J. Clin. Invest 2004;113:1328–1333. [PubMed: 15124024]

Berditchevski F. Complexes of tetraspanins with integrins: more than meets the eye. J. Cell. Sci 2001;114:4143–4151. [PubMed: 11739647]

Coillie EV, Damme JV, Opdenakker G. The MCP/eotaxin subfamily of CC chemokines. Cytokine Growth Factor Rev 1999;10:61–86. [PubMed: 10379912]

Creagh EM, Conroy H, Martin SJ. Caspase-activation pathways in apoptosis and immunity. Immunol. Rev 2003;193:10–21. [PubMed: 12752666]

Gao J, Gelber-Schwalb TA, Addeo JV, Stern ME. Apoptosis in the lacrimal gland and conjunctiva of dry eye dogs. Adv. Exp. Med. Biol 1998;438:453–460. [PubMed: 9634921]

Gao J, Schwalb TA, Addeo JV, Ghosn CR, Stern ME. The role of apoptosis in the pathogenesis of canine keratoconjunctivitis sicca: the effect of topical cyclosporin A therapy. Cornea 1998;17:654–663. [PubMed: 9820947]

Gudmundsson OG, Bjornsson J, Olafsdottir K, Bloch KJ, Allansmith MR, Sullivan DA. T cell populations in the lacrimal gland during aging. Acta Ophthalmol. (Copenh.) 1988;66(5):490–497. [PubMed: 3064534]

Hodges RR, Dartt DA. Regulatory pathways in lacrimal gland epithelium. Int. Rev. Cyt 2003;231:129–196.

Ishikawa H, Claudio E, Dambach D, Raventos-Suarez C, Bravo R. Chronic inflammation and susceptibility to bacterial infectious in mice lacking the polypeptide (p)105 precursor (NF-kB1) but expressing p50. J. Exp. Med 1998;187:985–996. [PubMed: 9529315]

Jenson SD, Robetorye RS, Bohling SD, Schumacher JA, Morgan JW, Lim MS, Elenitoba-Johnson KSJ. Validation of cDNA microarray gene expression data obtained from linearly amplified RNA. J. Clin. Pathol 2003;56:307–312.

King HC, Sinha AA. Gene expression profile analysis by DNA microarrays: promise and pitfalls. JAMA 2001;286:2280–2288. [PubMed: 11710894]

Lin L, DeMartino GN, Greene WC. Cotranslational dimerization of the Rel homology domain of NF-kappaB1 generates p50-p105 heterodimers and is required for effective p50 production. EMBO J 2000;19:4712–4722. [PubMed: 10970863]

Livak KJ, Schmittgen TD. Analysis of relative gene expression data using real-time quantitative PCR and the 2T−ΔΔC method. Methods 2001;25:402–408. [PubMed: 11846609]

Mircheff AK, Gierow JP, Lee LM, Lambert RW, Akashi RH, Hofman FM. Class II antigen expression by lacrimal epithelial cells. An updated working hypothesis for antigen presentation by epithelial cells. Invest. Ophthalmol. Visual Sci 1991;32:2302–2310. [PubMed: 1830042]

Nguyen, D.; Toshida, H.; Vadlamudi, V.; Akinyemi, O.; Beuerman, RW. Real-time PCR verification of microarray data in the rat lacrimal gland following parasympathetic denervation. Association for Research in Vision and Ophthalmology (ARVO) E-Abstract 1024. 2003. (www.arvo. org)

Nguyen DH, Toshida H, Schurr J, Beuerman RW. Microarray analysis of the rat lacrimal gland following the loss of parasympathetic control of secretion. Physiol. Genomics 2004;18:108–118. [PubMed: 15084711]

Nguyen, D.; Nhan, TL.; Toshida, H.; Pedroza, L.; Beuerman, RW. Loss of muscarinic, parasympathetic activation induces long-germ changes in proinflammatory and immune response gene expression in

the rat lacrimal gland. Association for Research in Vision and Ophthalmology (ARVO) E-Abstract 2418. 2005. (www.arvo.org)

Obata H, Yamamoto S, Horiuchi H, Machinami R. Histopathologic study of human lacrimal gland. Statistical analysis with special reference to aging. Ophthalmology 1995;102(4):678–686. [PubMed: 7724184]

Pflugfelder SC. Antiinflammatory therapy for dry eye. Am. J. Ophthalmol 2004;137:337–342. [PubMed: 14962426]

Radonić A, Thulke S, Mackay IM, Landt O, Siegert W, Nitsche A. Guideline to reference gene selection for quantitative real-time PCR. Biochem. Biophys. Res. Commun 2004;313:856–862. [PubMed: 14706621]

Raghavan M, Bjorkman PJ. Fc receptors and their interactions with immunoglobulins. Annu. Rev. Cell Dev. Biol 1996;12:181–220. [PubMed: 8970726]

Rajeevan MS, Ranamukhaarachchi DG, Vernon SD, Unger ER. Use of real-time quantitative PCR to validate the results of cDNA array and differential display PCR technologies. Methods 2001a; 25:443–451. [PubMed: 11846613]

Rajeevan MS, Vernon SD, Taysavang N, Unger ER. Validation of array-based gene expression profiles by real-time (kinetic) RT-PCR. J. Mol. Diagnostics 2001b;3:26–31.

Ramakers C, Ruijter JM, Deprez RH, Moorman AF. Assumption-free analysis of quantitative real-time polymerase chain reaction (PCR) data. Neurosci. Lett 2003;339:62–66. [PubMed: 12618301]

Rutkowski DT, Kaufman RJ. A trip to the ER: coping with stress. Trends Cell Biol 2004;14:61–63. [PubMed: 15106610]

Sabroe I, Lloyd CM, Whyte MKB, Dower SK, Williams TJ, Pease JE. Chemokines, innate and adaptive immunity, and respiratory diseases. Eur. Respir. J 2002;19:350–355. [PubMed: 11871367]

Slee EA, Harte MT, Kluck RM, Wolf BB, Casiano CA, Newmeyer DD, Wang HG, Reed JC, Nicholson DW, Alnemri ES, Green DR, Martin SJ. Ordering the cytochrome *c*-initiated caspase cascade: hierarchical activation of caspases-2, -3, -6, -7, -8 and -10 in a caspase-9-dependent manner. J. Cell Biol 1999;144:281–292. [PubMed: 9922454]

Solomon A, Dursun D, Liu Z, Xie Y, Macri A, Pflugfelder SC. Pro- and anti-inflammatory forms of interleukin-1 in the tear fluid and conjunctiva of patients with dry-eye disease. Invest. Ophthalmol. Visual Sci 2001;42:2283–2292.

Stern ME, Gao J, Siemasko KF, Beuerman RW, Pflugfelder SC. The role of the lacrimal functional unit in the pathophysiology of dry eye. Exp. Eye Res 2004;78:409–416. [PubMed: 15106920]

Strong B, Farley W, Stern ME, Pflugfelder SC. Topical cyclosporine inhibits conjunctival epithelial apoptosis in experimental murine keratoconjunctivitis sicca. Cornea 2005;24:80–85. [PubMed: 15604871]

Sullivan DA. Immunology of the lacrimal gland and tear film. Dev. Ophthalmol 1999;30:39–53. [PubMed: 10627915]

Toshida H, Beuerman RW. Effects of preganglionic parasympathetic denervation on the rabbit lacrimation. Adv. Exp. Med. Biol 2002;506:225–229. [PubMed: 12613912]

Tsubota K, Fujita H, Tsuzaka K, Takeuchi T. Quantitative analysis of lacrimal gland function, apoptotic figures, Fas and Fas ligand expression of lacrimal glands in dry eye patients. Exp. Eye Res 2003;76:233–240. [PubMed: 12565811]

Utans U, Arceci RJ, Yamashita Y, Russell ME. Cloning and characterization of allograft inflammatory factor-1: a novel macrophage factor identified in rat cardiac allografts with chronic rejection. J. Clin. Invest 1995;95:2954–2962. [PubMed: 7769138]

Walcott B, Cameron RH, Brink PR. The anatomy and innervation of lacrimal glands. Adv. Exp. Med. Biol 1994;350:11–18. [PubMed: 7913283]

Walker NJ. Tech. Sight. A technique whose time has come. Science 2002;296:557–559. [PubMed: 11964485]

Williams RM, Singh J, Sharkey KA. Innervation and mast cells of the rat exorbital lacrimal gland: the effects of age. J. Auton. Nerv. Syst 1994;47(12):95–108. [PubMed: 8188988]

Yeh S, Song XJ, Farley W, Li D, Stern ME, Pflugfelder SC. Apoptosis of ocular surface cells in experimentally induced dry eye. Invest. Ophthalmol. Visual Sci 2003;44:124–129. [PubMed: 12506064]

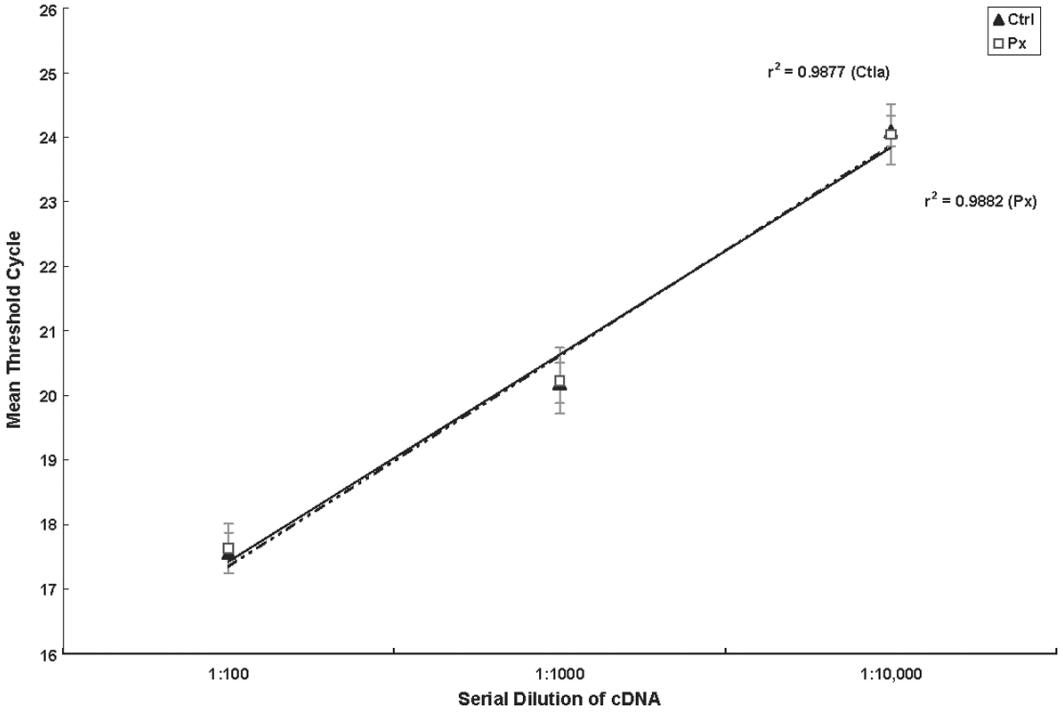

Fig. 1.

Linear regression plot of 18S rRNA MC_T data in the contralateral, unoperated control, and parasympathectomized lacrimal glands.

Table 1

Primer and probe sequences used for real-time PCR analysis

Gene name	Primers for real-time PCR (5′ to 3′)	Amplicon (bp)
Furin convertase		
Sense	CGAGAGGACCGCCTTTATCAAA	131
Antisense	GTCCAAACCCAGTCCCAAGATAA	
Protein disulfide isomerase (PDI)		
TaqMan Probe	6-FAM TGTCCCAGCAGCCCACATCTCCG BHQ-1	148
Sense	CCTGAACCCAAAACCTCGGT	
Antisense	GAAGAGACAGGTTTAAGTGTACGT	
UDP-galactose transporter related isozyme 1 (UDP-Gal)		
Sense	TATGCGGGCTCATTACCAAACA	101
Antisense	GCTCCCCAGTAAACAGGATCC	
Eotaxin		
TaqMan Probe	6-FAM TCCTGCTGCTCACGGCCACTTCCT BHQ-1	142
Sense	CACCATGCAGCTCTCCACAG	
Antisense	CAGTAGTGTGTTGGGGATCTTCTT	
Caspase-1 (interleukin-1β converting enzyme; ICE)		
TaqMan Probe	6-FAM CCACTCGGTCCAGGAAATGCGCCA BHQ-1	113
Sense	TCTAAGGGAGGACATCCTTTCTC	
Antisense	TGGGCTATTTCTAAAGGGCAAAAC	
Caspase-2 (Nedd2/Ich-1)		
Sense	CCCTTCTCGGTGTGTGAGTC	148
Antisense	GCTGGTAGTGTGCCTGGTAAA	
Caspase-6 (Mch2)		
Sense	GCAGTACAAGATGGACCACAAGA	143
Antisense	ATCCTAGCTCTGAGAACCTTCGA	
Leukocyte antigen MRC-OX44 (CD53)		
Sense	TGTGGTGTAAATGGCTCAAGTGA	143
Antisense	ACGCAGATGGTAACGATTCCAATA	
IgG receptor FcRn large subunit p51		
Sense	GCCATCTATGCGCCTGAAGG	149
Antisense	TGGGACCAGTGCTGCAATTC	
MHC class II antigen RT1.D alpha chain		
Sense	TAGGCATCGTCGTCGGGATT	90
Antisense	CGGTATCTCACAGGGCTCCTT	
MHC class II antigen RT1.B beta chain		
Sense	ACATCTACAACCGGGAGGAGTA	283
Antisense	GCTGGGTAGAAATCTGTCACTGA	
Lysosomal membrane glycoprotein 1 (LAMP-1)		
Sense	AAGCAAACAGGAGCAGGGAC	141
Antisense	CGGCAGAGCACAGAAACACT	
Macrophage metalloelastase (MME)		

Gene name	Primers for real-time PCR (5′ to 3′)	Amplicon (bp)
Sense	TGAAAGGAGCTGGCACAATGAA	259
Antisense	TTCAGAGTTGAGGTGTCCAGTTG	
Nuclear factor kappa beta p105 (NF-κB1)		
Sense	CAAGCAGGAAGATGTGGTGGA	109
Antisense	ATCATGTCCTTCTTTGGCAGCTA	
Lysosomal acid lipase (LAL)		
Sense	GGCGGAAGAACCAGTTTGATAAAG	104
Antisense	GTTGTCAATGTTTGTGACCCAGTT	
Proteasome subunit, beta type 4 (PSMB4)		
Sense	GCTATCCATTCATGGTTGACAAGG	96
Antisense	TCCACCAGCATAGCCTCCAA	
Proteasome subunit RC1 (PSMB8, LMP7)		
Sense	CCAGGAAAGGAAGGTTCAGATTGA	87
Antisense	TCTACAGCCACGATGACTCCAT	
Allograft inflammatory factor-1 (AIF-1)		
Sense	GCGAATGCTGGAGAAACTTGG	110
Antisense	TGAGAAAGTCAGAGTAACTGAACG	
Muscarinic acetylcholine receptor subtype 3 (M_3R)		
Sense	GCAAGACCTCTGACACCAACT	92
Antisense	AGCAAACCTCTTAGCCAGCG	
18S ribosomal RNA (18S rRNA)		
Sense	CATTCGAACGTCTGCCCTATCA	162
Antisense	GGGTCGGGAGTGGGTAATTTG	

Table 2

MC_T data for genes tested using real-time PCR at 7 days after GSPN sectioning

Accession number	Gene name	Ctla MC_T±S.E.M.	P_X MC_T±S.E.M.	*t*-test
Protein processing				
X55660	Furin convertase	22.88±0.78	24.00±0.89	0.00169
X02918	Protein disulfide isomerase (PDI)	21.33±0.35	21.75±0.33	0.03483
D87991	UDP-galactose transporter related isozyme 1 (UDP-Gal)	22.86±0.25	24.07±0.78	0.00001
NM_012857	Lysosomal membrane glycoprotein 1 (LAMP-1)	28.84±0.84	28.71±1.00	0.91983
S81497	Lysosomal acid lipase (LAL)	31.10±0.65	29.96±0.51	0.18515
NM_031629	Proteasome subunit, beta type 4 (PSMB4)	22.74±0.33	22.52±0.18	0.56704
D10729	Proteasome subunit RC1 (PSMB8, LMP7)	32.61±0.00	32.02±0.00	0.60938
Pro-inflammatory and pro-apoptotic				
Y08358	Eotaxin	28.20±0.33	27.28±0.54	0.00004
U14647	Caspase-1	30.21±0.41	29.04±0.55	0.00113
U77933	Caspase-2 (Nedd2/Ich-1)	29.03±0.66	27.55±0.43	0.00116
AF025670	Caspase-6 (Mch2)	31.61±0.33	31.13±0.34	0.03208
M57276	Leukocyte antigen MRC-OX44 (CD53)	32.71±0.29	30.29±0.22	0.00001
X14323	IgG receptor FcRn large subunit p51	33.57±0.15	32.02±0.27	0.00001
Y00480	MHC class II antigen RT1.D alpha chain	30.59±0.21	29.36±0.35	0.00801
M36151	MHC class II antigen RT1.B beta chain	35.00±0.46	32.35±0.53	0.00246
X98517	Macrophage metalloelastase (MME)	34.78±0.73	33.01±0.00	0.04162
L26267	Nuclear factor kappa beta p105 (NF-κB)	31.99±0.43	30.37±0.16	0.00172
U17919	Allograft inflammatory factor-1 (AIF-1)	31.62±0.36	29.18±0.36	0.00021
Other				
AB017656	Muscarinic acetylcholine receptor subtype 3 (M_3R)	26.70±0.28	26.78±0.57	0.13447

Ctla, contralateral unoperated control side; Px, parasympathectomized side.

Table 3

MC_T data for 18S rRNA over serial dilutions of cDNA using real-time PCR

18S rRNA (accession no. V01270)	Ctla MC_T±S.E.M.	Px MC_T±S.E.M.	*t*-test
1:100 dilution	17.56±0.32	17.63±0.38	0.17910
1:1000 dilution	20.19±0.31	20.23±0.51	0.22991
1:10,000 dilution	24.08±0.24	24.04±0.47	0.92789

Ctla, contralateral unoperated control side; Px, parasympathectomized side.

Table 4

Validation of DNA microarray results by real-time PCR at 7 days after GSPN sectioning

Accession number	Gene name	Fold change		Validation
		DNA microarray	Real-time PCR	
Protein processing				
X55660	Furin convertase	-2.1	-4.3	Y
X02918	Protein disulfide isomerase (PDI)	-2.4	-2.8	Y
D87991	UDP-galactose transporter related isozyme 1 (UDP-Gal)	-2.3	-2.4	Y
NM_012857	Lysosomal membrane glycoprotein 1 (LAMP-1)	2.6	1.5	N
S81497	Lysosomal acid lipase (LAL)	5.9	1.9	N
NM_031629	Proteasome subunit, beta type 4 (PSMB4)	1.3	1.2	N
D10729	Proteasome subunit RC1 (PSMB8, LMP7)	1.9	1.4	N
Pro-inflammatory and pro-apoptotic				
Y08358	Eotaxin	4.3	2.6	Y
U14647	Caspase-1	5.5	3.5	Y
U77933	Caspase-2 (Nedd2/Ich-1)	2.3	2.3	Y
AF025670	Caspase-6 (Mch2)	2.1	1.3	N
M57276	Leukocyte antigen MRC-OX44 (CD53)	2.0	4.6	Y
X14323	IgG receptor FcRn large subunit p51	2.3	2.9	Y
Y00480	MHC class II antigen RT1.D alpha chain	2.5	2.4	Y
M36151	MHC class II antigen RT1.B beta chain	1.6	2.0	Y
X98517	Macrophage metalloelastase (MME)	2.4	4.8	Y
L26267	Nuclear factor kappa beta p105 (NF-κB1)	1.7	2.7	Y
U17919	Allograft inflammatory factor-1 (AIF-1)	2.2	4.7	Y
Other				
AB017656	Muscarinic acetylcholine receptor subtype 3 (M_3R)	-1.0	-1.3	Y

Table 5

Real-time PCR results of pro-inflammatory gene expression at 2.5 months after GSPN sectioning

Gene name	Fold change		Change
	7 Days	2.5 Months	
Pro-inflammatory and pro-apoptotic			
Caspase-1	3.5	3.9	NC
IgG receptor FcRn large subunit p51	2.9	3.4	NC
MHC class II antigen RT1.D alpha chain	2.4	6.6	I
MHC class II antigen RT1.B beta chain	2.0	6.6	I
Macrophage metalloelastase	4.8	4.5	NC
Nuclear factor kappa beta p105	2.7	2.3	NC
Allograft inflammatory factor-1	4.7	4.1	NC

The results show a persistent increase in intracellular mediators of inflammation that may lead to initiation of autoimmunity in the denervated LG. The “Change” call of Increase (I) or Decrease (D) is indicated if the difference between the fold changes at 7 days and 2.5 months is greater than 2-fold. NC, no change.